High-capacity glycol chitosan-based nanoemulsion for efficient delivery of disulfiram

Q1 Q2

Erazuliana Abd Kadir[a,b,*], erazuliana@usm.my, Ijeoma F. Uchegbu[a], Andreas G. Schätzlein[*,a,**], a.schatzlein@ucl.ac.uk

[a]UCL School of Pharmacy, 29-39 Brunswick Square, London WC1N 1AX, UK

[b]Department of Toxicology, Advanced Medical & Dental Institute, Universiti Sains Malaysia, 13200, Kepala Batas, Pulau Pinang, Malaysia

*Corresponding author at: UCL School of Pharmacy, 29-39 Brunswick Square, London WC1N 1AX, UK. Corresponding author at: Department of Toxicology, Advanced Medical & Dental Institute, Universiti Sains Malaysia, 13200, Kepala Batas, Pulau Pinang, Malaysia

**Corresponding author at: UCL School of Pharmacy, 29-39 Brunswick Square, London, WC1N 1AX, UK

> Author has made corrections in ce:affiliation. Carry out the corrections in sa:affiliation also using the XML Editor.

Abstract

Disulfiram (DS) is an anti-alcoholism drug capable of acting against important and hard-to-treat cancers. The drug's relative instability and variable absorption/distribution have led to its variable pharmacokinetics and suboptimal exposure. Hence, it was hypothesised that a nano-enabled form of DS might be able to overcome such limitations. Encapsulation of the labile DS was achieved with quaternary ammonium palmitoyl glycol chitosan (GCPQ) to form a high-capacity, soybean oil-based DS-GCPQ nanoemulsion. DS-GCPQ showed capability of oil-loading up to 50% v/v for a stable entrapment of high drug content. With increasing oil content (10 to 50% v/v), the mean particle size and polydispersity index were also increased (166 to 351 nm and 0.14 to 0.22, respectively) for a given amount of GCPQ. Formulations showed a highly positive particle surface charge (50.9 ± 1.3 mV), contributing to the colloidal stability of the individual particles. DS-GCPQ showed marked cytotoxicity against pancreatic cancer cell lines with enhanced activity in the presence of copper. An intravenous pharmacokinetic study of DS-GCPQ *in vivo* showed improved plasma drug stability with a DS half-life of 17 min. Prolonged survival was seen in tumour-bearing animals treated with DS-GCPQ supplemented with copper. In conclusion, DS-GCPQ nanoemulsion has the potential to be developed further for cancer therapeutic purposes.

Keywords:

Disulfiram, Nanoemulsion, GCPQ, Pharmacokinetic, Anticancer

Abbreviations

No keyword abbreviations are available

Data availability

Data will be made available on request.

1 Introduction

With 10 million cancer-related deaths worldwide reported in 2020 (Sung et al., 2021), the search for safe and potent anticancer drugs capable of selectively killing cancer cells without harming normal cells continues. Apart from the

development of novel chemical entities, there is also considerable interest in repurposing, i.e. exploring the anticancer potential of existing drugs with known safety profiles.

Disulfiram (DS) has been used for the treatment of alcoholism since the year of 1947 (Chick, 1999) and was the first medication approved by U.S. Food and Drug Administration (FDA) for the treatment of chronic alcohol dependence. Recently, DS has been discovered to have activities against cancer and therefore sparked an interest among researchers to repurpose DS into an anticancer drug. Both *in vitro* and *in vivo* studies have reported that DS has cytotoxic effects against several types of cancer, such as pancreatic (Kim et al., 2013; Xu et al., 2021), breast (Chen et al., 2006; Liu et al., 2014; Swetha et al., 2020), brain (Qu et al., 2021; Yang et al., 2022), prostate (Lin et al., 2011), lung (Duan et al., 2014; Nechushtan et al., 2015) and skin cancer (Meraz-Torres et al., 2020). The anticancer property of DS is heightened when given to the patients in combination with metal, in particular, copper (Kannappan et al., 2021).

The main mechanism of action of DS as an anti-alcoholic drug is by inhibiting aldehyde dehydrogenase (ALDH) from converting acetaldehyde to acetate in the metabolism of alcohol. Accumulation of acetaldehyde causes uncomfortable side effects such as sweating and flushing on the upper chest and face (flush syndrome), nausea, vomiting, tachycardia, vertigo and blurred vision (Wright and Moore, 1990), thus encouraging the abstinence towards drinking alcohol. In recent years, ALDH has been linked to cancer through its function as a cancer marker. The ALDH1-positive tumours were associated with poor clinical prognosis of breast, pancreatic and lung cancer (Ginestier et al., 2007; Jiang et al., 2009; Marcato et al., 2011; Rasheed et al., 2010). The ALDH2, an important enzyme in acetaldehyde oxidation, was linked to alcohol-mediated carcinogenesis (Seitz and Stickel, 2007). The specific property of DS in blocking the activity of ALDH enzyme could have contributed to its role as an anticancer agent, thus making it a strong candidate for use as an adjuvant in chemotherapeutic treatments.

A potential reason DS has not been used widely in clinical applications for cancer treatment is probably due to the absence of a DS formulation that could prolong the short half-life of the drug in the acidic gastric fluid. It is crucial to prevent DS from decomposing into diethylamine and carbon disulphide upon oral consumption (Johansson, 1992). There is also a lack of DS formulation that could protect DS from rapid degradation in blood circulation from the activity of glutathione reductase and interactions with endogenous enzymes (Eneanya et al., 1981; Johansson, 1992). Despite the labile nature of DS, its metabolism pathway in humans is well-known, thus ensuring the safety of DS usage to be used in larger dosages, which gives a distinct advantage in repurposing DS as a chemotherapy drug.

Acid degradation of glycol chitosan (GC) followed by conjugation of palmitoyl groups and quaternisation of amine residues creates positively charged amphiphilic polymer GCPQ, which spontaneously self-assembles to form micelles in an aqueous solution. Encapsulation of hydrophobic drugs within these GCPQ micelles can protect the drug from gastric and intestinal degradation and could improve absorption in the gut (Lalatsa et al., 2012b). GCPQ is bioadhesive, allowing adherence of the GCPQ-based nanoparticles to the mucus membrane, thus providing a longer residence time of the drug in the gut for a higher chance of absorption through the gut wall (Siew et al., 2012). The nanometre size range of GCPQ nanoparticles creates a high surface area which potentially facilitates faster drug dissolution (Lalatsa et al., 2012a). GCPQ can be loaded with hydrophobic drugs such as griseofulvin, cyclosporine and propofol by mixing in an aqueous media (Qu et al., 2006; Siew et al., 2012).

It was hypothesised that GCPQ would encapsulate the hydrophobic DS and stabilise the structure of the nanoparticles. Fundamental approaches were taken to produce stable and robust GCPQ-based nanoemulsions, including thorough formulation characterisation *in vitro* and *in vivo* to ensure the optimum criteria of nanoparticles were achieved.

2 Materials

All chemicals and reagents were obtained from Sigma-Aldrich Co. Ltd., Dorset, UK, unless otherwise stated. All solvents were obtained from Fisher Scientific Ltd., Leicestershire, UK. Disulfiram and S-methyl-N,N-diethyldithiocarbamate (MeDDC) were purchased from Santa Cruz Biotechnology, Inc., California, USA. Deuterated methanol was obtained from Cambridge Isotope Laboratories Inc., Massachusetts, USA. The human pancreatic cancer cell line (MIAPaCa-2) was obtained from American Type Culture Collection, Rockville, Maryland, USA. Glucose IV infusion was obtained from Hameln Pharmaceuticals Limited, Gloucester, UK.

3 Methods

3.1 Synthesis of GCPQ

GCPQ was synthesised as described previously (Siew et al., 2012; Uchegbu et al., 2001). Briefly, 2 g of GC was dissolved in 152 ml 4 M hydrochloric acid and incubated in a 50 °C water bath with shaking at 125 rpm for 24 h. After 24 h, the degraded GC (dGC) solution was cooled to room temperature (RT) and transferred into seamless cellulose dialysis tubes (MWCO 3.5 kDa) for dialysis against 5 L of distilled water with six changes of the water in 24 h. The dialysate was then freeze-dried until a white, cotton-like solid was obtained. Every 500 mg dGC was dissolved in 24 ml absolute ethanol and 76 ml Milli-Q water pre-added with 376 mg sodium bicarbonate, followed by drop-by-drop addition of 792 mg palmitic acid N-hydroxysuccinimide ester (PNS) pre-dissolved in 150 ml absolute

ethanol into the dissolved dGC solution. The palmitoylation process was performed under the protection of light and continuous stirring for 72 h. Ethanol in the cloudy mixture of palmitoylated GC (PGC) was later removed using a rotary evaporator at 50 to 52 °C under reduced atmospheric pressure. The remaining aqueous phase was then extracted with diethyl ether (three times the volume of the aqueous phase). The cloudy aqueous mixture was dialysed exhaustively against water (5L) using a dialysis membrane (MWCO 12–14 kDa) with 6 changes of water in 24 h. The dialysate (PGC) was freeze-dried to give a cotton-like solid. Every 300 mg PGC was dispersed in 25 ml N-methyl-2-pyrrolidone (NMP) overnight with continuous stirring. Later, 45 mg sodium iodide, 0.44 ml methyl iodide and 40 mg sodium hydroxide pre-dissolved in 4 ml absolute ethanol were added into the PGC dispersion and continuously stirred at 36 °C under a nitrogen atmosphere for 3 h. The product (GCPQ) was obtained by precipitation with diethyl ether. The resultant solid product was dissolved in 100 ml water (for every 400 mg PGC) and dialysed exhaustively against water (5L) using a dialysis membrane (MWCO 7 kDa) with 6 changes of water over 24 h. For the removal of iodide from the product, the dialysate was passed through a column made of 100 ml Amberlite IRA-96 (pre-washed with 150 ml 1 M hydrochloric acid, followed by a copious amount of Milli-Q water until a neutral pH was obtained). The brown eluate was then freeze-dried to give a cotton-like GCPQ product.

3.2 Characterisation of GCPQ

Characterisation of GCPQ involved determination of a) molecular weight of the polymer using gel permeation chromatography and multiangle laser light scattering, and b) percentage of palmitoylation and quaternisation using proton nuclear magnetic resonance (^{1}H NMR) analysis, as described previously (Lalatsa et al., 2015; Serrano et al., 2015; Siew et al., 2012).

3.3 Formulation of DS-GCPQ

The DS-GCPQ nanoemulsions were made at 1 to 10 drug-to-polymer ratio (w/w) in 1 ml volume. The stock of DS in soybean oil (SBO) was prepared at 20 mg/ml by dissolving DS crystals in the oil at 50 °C and cooled to room temperature (RT) before use. GCPQ was dissolved in Milli-Q water at 10 mg/ml prior to the addition of DS in SBO. Formulations containing either 5, 10, 20, 30, 40 or 50% oil v/v were prepared by adding either 50, 100, 200, 300, 400 or 500 µl DS in SBO into 10 mg/ml GCPQ suspension at either 950, 900, 800, 700, 600 or 500 µl volumes, respectively. The final volume for all different oil content formulations was 1 ml. The formulations were then sonicated using an ultrasonic disintegrator at amplitude 5 (Soniprep 150 Plus, MSE, U.K.) for 15 min.

3.4 Characterisation of DS-GCPQ

3.4.1 Drug content

The drug content of the formulations was analysed using high-performance liquid chromatography (HPLC) equipped with one reverse phase Phenomenex Onyx Monolithic C18 column (4.6 × 100 mm) connected with a guard column (4.6 × 5 mm) on Agilent 1200 series HPLC (Agilent Technologies, Wokingham, UK) with a quaternary pump, degasser, autosampler and UV detector. The mobile phase was a mixture of methanol and Milli-Q water at an 80:20 v/v ratio. The flow rate was 1.0 ml/min with column temperature at 30 °C and injection volume of 5 µl. The DS peak was measured at wavelength 275 nm with a retention time of 1.58 min. The amount of DS encapsulated in the nanoparticles was determined as drug entrapment (DE%) which represents the percentage of the amount of drug found (drug content) in proportion to the amount of drug added into the formulation.

3.4.2 Particle size, polydispersity and surface charge

Dynamic light scattering (DLS) analysis was used to measure the particle size, polydispersity index (PDI) and zeta potential (surface charge) of the nanoparticle formulations. The DLS analysis was performed using Malvern Zetasizer Nano ZS ZEN3600 (Malvern Instruments Ltd., Worcestershire, UK) fitted with a 633 nm (red) laser. The sample was prepared by diluting 10 µl formulation in 990 µl Milli-Q water to meet data quality criteria set by the DLS equipment.

3.4.3 Transmission electron microscope (TEM)

Preparation of the samples for TEM imaging was performed by placing a small amount of the nanoparticle formulation (±10 µl) on a carbon-coated grid and negatively stained with uranyl acetate (1% w/v). Images of the samples were then captured using FEI CM129 BioTwin transmission electron microscope (Philips, Eindhoven, The Netherlands) fitted with an advanced microscopy technique digital camera.

3.5 Stability of DS-GCPQ

The effects of changes in bulk pH, presence of salts and gastrointestinal enzymes on the morphology and drug encapsulation of the nanoparticles were determined by exposing the freshly prepared DS-GCPQ nanoemulsions at 5% oil content to either highly acidic or basic pH solution, buffers, or simulated biological medium of the gastric and intestinal fluid, respectively.

3.5.1 Stability in acidic and basic pH

DS-GCPQ nanoemulsion and 10 mg/ml GCPQ aqueous suspension (control) were titrated with either 0.1 M hydrochloric acid (HCl) or 0.1 M sodium hydroxide (NaOH) solution to expose a highly acidic (pH 1.7) or highly basic (pH 11) condition to the nanoparticles, respectively. Both formulation and control were then sampled immediately for particle size and PDI measurement.

3.5.2 Stability in buffer

HCl buffer at pH 1.2 was prepared by mixing 50 ml 0.2 M potassium chloride, 85 ml 0.2 M HCl solution and 65 ml Milli-Q water in a 200 ml volumetric flask. Phosphate buffer at pH 6.8 was prepared by mixing 50 ml 0.2 M monobasic potassium phosphate, 22.4 ml 0.2 M NaOH solution and 127.6 ml Milli-Q water in a 200-ml volumetric flask. The stability of DS-GCPQ in the buffer was determined by assessing the DE% of the formulation in the buffer at various time points.

The DS-GCPQ formulation was added into either HCl or phosphate buffer solutions (1:9 ratio) at RT (22–24 °C). Samples were taken (50 µl) at 0 min (right after addition), 30 min, 1, 2 and 4 h after the addition of the formulation into the buffer (t = 0, 0.5, 1, 2 and 4, respectively), followed by dilution with 950 µl ethanol. The samples were then centrifuged at 1,000 g for 10 min to sediment any large particles (e.g., salt crystals) that may be present in the samples. The drug content in the supernatant was then measured with HPLC.

3.5.3 Stability in simulated biological samples

Simulated gastric fluid (SGF) and simulated intestinal fluid (SIF) were prepared as described in British Pharmacopoeia (2013). SGF which consisted of 2 g sodium chloride and 3.2 g pepsin powder was later added with 80 ml 1 M HCl to make 1 L of SGF solution at pH 1.2. In contrast, SIF consisted of 77 ml of 0.2 M sodium hydroxide, 250 ml of 6.8 g potassium dihydrogen phosphate and 10 g of pancreas powder to make 1 L of SIF solution at pH 6.8. For control, 1 mg/ml of DS was prepared in 2% dimethyl sulfoxide (DMSO). An amount of 400 µl of the DS-GCPQ 5% oil formulations or control was added into 3.6 ml of either SGF or SIF and incubated in a 37 °C water bath. The drug content was assessed at several time points after the addition of formulation into either SGF or SIF; right after the addition of formulation (t = 0), and at 30 min, 1 h, 2 h and 4 h post-addition (t = 0.5, 1, 2 and 4, respectively). At each time point, 50 µl of either SGF or SIF solutions were taken and diluted in 950 µl ethanol. The samples were then centrifuged at 1,000 g for 10 min. The supernatant was collected and subjected to HPLC analysis.

3.5.4 Stability in mouse plasma

Mouse plasma diluted to 50% of the initial concentration using 0.9% w/v sodium chloride solution was prepared in bulk (approximately 8 ml) before the experiment. An amount of 995 µl of the diluted plasma was placed in a microcentrifuge tube and placed in a 37 °C water bath for at least 30 min. Once the plasma temperature stabilised, 5 µl of either DS-GCPQ at 5% oil or 1 mg/ml DS solution in 0.5% DMSO was added into the plasma (n = 3). The samples were maintained in a 37 °C water bath throughout the experiment. Samples were measured for drug content at time points 0, 10, 30, 60 and 120 min using LC-MS/MS analysis (see 3.7.2).

3.6 DS-GCPQ activity against cancer cells

The anticancer activity of DS and DS-GCPQ, with and without the presence of copper against the human pancreatic cancer cell line MIAPaCa-2, was determined using thiazolyl blue tetrazolium bromide (MTT) reduction assay.

3.6.1 Cell culture condition

Freshly thawed MIAPaCa-2 (ATCC® CRL-1420™, Manassas, VA, USA) cells from cryopreservation were grown for at least 2 weeks prior to the experiment. The complete growth medium used for the cells was prepared using sterile-filtered Dulbecco's Modified Eagle's Medium (DMEM) added with 10% v/v fetal bovine serum (FBS) and 1 mM sodium pyruvate. The cells were maintained in a CO_2 incubator with an environment set at 5% CO_2 and 37 °C temperature.

3.6.2 Cytotoxicity assay

Cells were seeded at 500 cells in 200 µl medium per well in 96-well plates and incubated in the CO_2 incubator for 3 days to allow the cells to be in the log phase growth during the treatment. The cells were treated with four different types of treatments: 1) DS in 2% DMSO (DS), 2) DS-GCPQ at 5% oil content (DS-GCPQ), 3) DS in 2% DMSO with copper chloride ($CuCl_2$) (DS + Cu) and 4) DS-GCPQ at 5% oil content with $CuCl_2$ (DS-GCPQ + Cu). $CuCl_2$ solution was prepared in phosphate buffered saline (PBS) at a concentration equimolar to the DS molarity (1 mg DS = 3.37×10^{-6} mol = 0.45 mg $CuCl_2$). Ten different concentrations for each type of treatment were achieved by serial dilution from 500 to 5×10^7 µg/ml DS. The cells were incubated with the treatments for 4 h. For positive control, cells were treated with 200 µl of 1% Triton-X solution for 10 min. After the drug incubation, cells were washed three times with PBS before adding 200 µl/well of fresh growth medium for incubation overnight. The cells were then incubated

with 200 μl of MTT solution (0.5 mg/ml) for 2 h in the incubator, protected from light. The formation of purple formazan crystals was confirmed with examination under a light microscope. The MTT solution was removed and 100 μl DMSO was added per well to dissolve the crystals. The absorbance was then measured using ELX808TM Absorbance Microplate Reader (Bio-TEK Instruments Inc., Winooski, Vermont, USA) at wavelength 570 nm. The cytotoxicity effect of the treatments was expressed as a percentage of cell survival (V%). The mean values of V% for each concentration were used to create a dose–response curve for determining half-maximal inhibitory concentration (IC_{50}) for each treatment.

3.7 Pharmacokinetic study of DsS-GepqCPQ

3.7.1 Animals

The animal experiments were approved by the local ethics committee and carried out under license from the UK Home Office and by the policies and regulations compliant with the Animals and Scientific Acts 1986 UK. All animals were housed at Biological Service Unit (BSU) and animal handling and care for scientific research were implemented as recommended by the UCL BSU guidelines.

Female CD-1 mice (Charles River, Kent, UK), 17–21 g, were maintained in controlled room conditions with ambient temperature at 22–25 °C, relative humidity at 55–60% and 12-hour light and dark cycles. Food and water were given *ad libitum* to the animals. All animals were acclimatised for a week before the experiment.

3.7.2 LcC-MsS/MsS analysis

3.7.2.1 Instrumentation and analytical conditions

The liquid chromatography-tandem mass spectrometry (LC-MS/MS) analysis was conducted using Agilent 1260 Infinity LC (Agilent Technologies, California, USA) connected to Agilent 6460 Triple Quadrupole LC/MS system with an ESI source equipped with Agilent Jet Stream technology. The chromatographic separations were performed using Phenomenex Onyx^{TM} Monolithic C18 analytical column (50 × 2 mm, 130 Å) connected to Phenomenex Onyx^{TM} Monolithic C18 guard column (5 × 2 mm, 130 Å) (Phenomenex, Torrance, California, USA). The column temperature was maintained at 30 °C. The LC run was carried out by injecting 5 μl of sample into the mobile phase of water added with 0.1% formic acid (A) and acetonitrile (B) under gradient elution of 5-minute runtime. The gradient conditions were as follows: B was increased from 5 to 95% at 1 min and stayed at the same value for 1.5 min. At 2.5 min, B was decreased back to 5% to be at the original ratio for re-equilibration of the column until stop time at 5 min. The flow was kept constant at 0.4 ml/min. The tandem mass spectrometry was done under positive ion mode. The source parameters were as follows: nitrogen as collision gas, the gas temperature at 300 °C, gas flow at 5 L/min, nebuliser at 45 psi, sheath gas heater and gas flow at 250 °C and 11 L/min, respectively and capillary voltage at 3.5 kV. Detection of the analytes was carried out using multiple reaction monitoring (MRM) scan type to monitor transitions of precursor-product ion of DS at m/z 297.1 > 116.1, MeDDC at m/z 164.06 > 116, and diphenhydramine hydrochloride (DPH) as the internal standard (IS) at m/z 256 > 167 with fragmentor voltage at 73 V for both DS and DPH and 45 V for MeDDC and collision energy 9 V for all analytes.

3.7.2.2 Preparation of cold stabilising agent

For 10 ml of stabilising agent, 90 mg of sodium chloride, 64 mg of sodium acetate, and 80 mg of diethylene triamine pentaacetic acid (DTPA) were mixed in 10 ml of Milli-Q water and stirred until all substances dissolved. The stabilising agent was ensured at pH 4.5 and kept at 4 0C °C until use.

3.7.3 Intravenous administration of DsS-GepqCPQ

Twenty-five female CD-1 mice were given single intravenous (IV) administration of DS-GCPQ at 20% oil content (4 mg/ml DS) in 5% glucose solution at a dosage of 20 mg/kg via the tail vein injection. Animals were then euthanised at 5 different time points (n = 5 per time point): 5 min, 15 min, 30 min, 1 h and 2 h by CO_2 asphyxiation.

Blood was immediately taken by cardiac puncture and collected into K_2EDTA blood tubes. The blood was then added with an equal volume of cold stabilising agent and centrifuged for 5 min at 10,000 g to obtain the stabilised plasma. The plasma was added with methanol (3 times the volume of plasma) containing the IS and vortexed vigorously for 10 min for drug extraction, followed by centrifugation at 10,000 g for 5 min to precipitate the protein. The methanol supernatant was collected without disturbing the pellet and kept on dry ice until the LC-MS/MS analysis. The samples were brought to room temperature 5 min before sampling. Pharmacokinetic parameters were determined using PK solver software (Zhang et al., 2010) with the implementation of non-compartmental analysis. Pharmacokinetic parameters were used to evaluate the treatments; elimination half-life ($t_{1/2}$), T_{max}, C_{max}, area under curve (AUC) and AUC_{0-t} where the AUC was measured from zero (0) hour to time of last quantifiable concentration (t).

3.8 Anticancer property of DsS-GepqCPQ

3.8.1 Animals

The animal experiments were carried out under ethical approval from the Home Office, as described previously in 23.7.1. Fifteen female CD-1 nude mice (Charles River, Kent, UK) of 17–21 g were kept in individually ventilated cages with constant temperature and humidity monitoring according to the UCL School of Pharmacy BSU guidelines. Animals were acclimatised for a week before the start of the experiment and were given food and water *ad libitum*.

3.8.2 Cell preparation and xenograft implantation

As described previously in 3.6.1, MIAPaCa-2 cells were grown for at least 2 weeks in the complete DMEM growth medium before the implantation. Cells for the implantation were prepared in a combination of blank growth medium (DMEM medium without FBS and sodium pyruvate) and Matrigel (Corning, New York, USA). The complete growth medium was first removed from the cells by centrifugation at 1000–2000 g for 3 min at 4 ℃ and replaced with a new blank growth medium. This step was repeated twice. Later, cells in the medium were mixed with liquid Matrigel at a 1:1 ratio containing 2×10^7 cells/ml and kept on ice until injection. The cell mixture was injected subcutaneously into the right flank of the mouse at 100 μl volume per flank. The day of implantation was determined as Day 0. The animals were monitored daily for the first tumour appearance, bodyweight change and health conditions. Once tumours were detected in all mice, animals were randomly divided into 3 groups (n = 5).

3.8.3 DsS-GepqCPQ and DS treatments in xenograft-implanted mice

Treatment was started when the tumour reached a palpable size of approximately 6–7 mm in diameter. Group 1 was the control group (no treatment), Group 2 was for the treatment of IV 20 mg/kg DS-GCPQ at 20% oil content in 5% glucose (IV DS-GCPQ), and oral 11.4 mg/kg copper gluconate (Oral Cu), and Group 3 was for the treatment of oral 20 mg/kg DS in SB oil (Oral DS) with Oral Cu. Treatments were given once every two days, along with the subsequent monitoring of the animals' tumour growth and body weight. Treatments were terminated in all groups once the total amount of 10 IV injections was given to the mice in Group 2. The tumour growth was continuously measured until it reached a maximum diameter of 13 mm, at which point the study was terminated. Mice were euthanised with CO_2 asphyxiation. The tumours were then excised and measured for tumour volume. The tumour volume (mm^3) was calculated as $(width^2 \times length)/2$.

3.9 Statistical analysis

Statistical analysis was performed using IBM SPSS Statistics for Windows, Version 22.0 (IBM Corp, Armonk, New York, USA). Comparison of more than two groups was done using One-way ANOVA with Tukey's multiple comparison test for the post-hoc analysis, whereas comparison between two groups was done using Independent samples *t*-test (Student's *t*-test). Survival data analysis was performed using GraphPad Prism version 5.00 for Windows (GraphPad Software, San Diego, California, USA). The survival of animals was determined using Kaplan-Meier analysis with Log rank (Mantel-Cox) test to compare two survival curves. Data were presented as mean ± standard deviation with significance value of $p < 0.05$.

4 Results

4.1 GepqCPQ polymer

GCPQ was synthesised, and the characteristics were as follows: M_w = 24,890 Da, M_n = 20,110 Da, M_w/M_n = 1.238, dn/dc = 0.140 ± 0.005 ml/g, mole % palmitoyl groups = 19.9, mole % quaternary ammonium groups = 11.2 ([Fig. S1](#) in [Supplementary Information](#)).

4.2 DsS-GepqCPQ nanoemulsion

The resulting dispersion of DS-GCPQ nanoemulsion was uniform and milky white in colour ([Fig. 1](#)). As GCPQ can act as a surfactant or emulsifier itself, no additional surfactant was added to stabilise the formulations. Formulations at 5, 10, 20, 30, 40 and 50% oil content were made to contain 1, 2, 4, 6, 8 and 10 mg/ml DS, respectively.
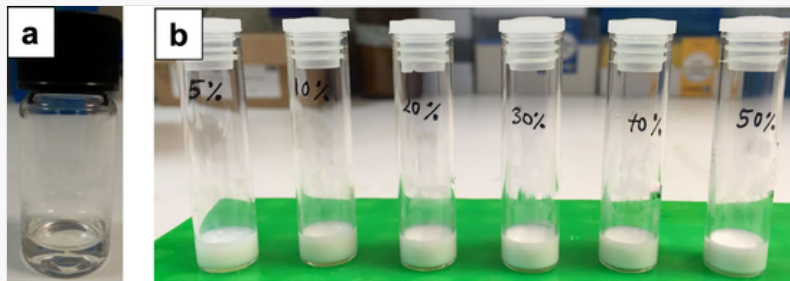
(i) Images are optimised for fast web viewing. Click on the image to view the original version.

Fig. 1

(a) GCPQ micelles appeared as a clear suspension. (b) The milky-white appearance of freshly prepared DS-GCPQ formulations at (from left) 5, 10, 20, 30, 40 and 50% v/v oil content. The formulations appeared thicker and denser towards the higher amount of oil content.

The drug content graph shows the trend of an increasing amount of DS detected towards the increasing amount of oil added into the formulations (Fig. 2a). This drug content was later interpreted into DE% to determine the encapsulation efficiency of GCPQ polymer on the different amounts of oil (Fig. 2b). The result shows all formulations having almost 100% drug entrapment with no significant difference of entrapment percentage between the different oil content formulations ($p > 0.05$). The particle size was in the range of 166 to 351 nm and was seen to increase with a higher amount of oil in the formulation (Fig. 2c). The mean particle size was found to be significantly different among the different oil content formulations ($p < 0.05$). On the other hand, all formulations showed low PDI (<0.3), albeit the values for 5% oil were significantly higher than 10 and 20% oil formulations and 40% oil was significantly higher than 10% oil formulations (Fig. 2d). The zeta potential of DS-GCPQ nanoemulsions (5% oil content) was 50.9 ± 1.3 mV at pH 4.54.

Fig. 2
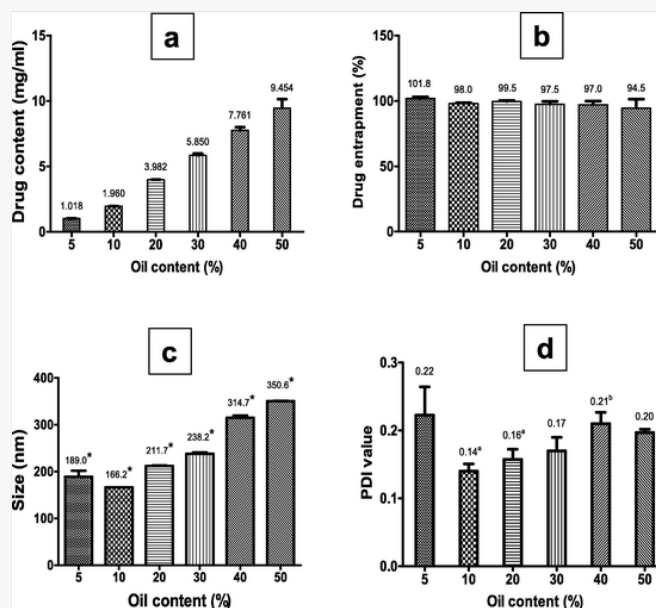
The bar graphs display the drug content (a), DE% (b), particle size (c) and PDI values (d) for the freshly prepared DS-GCPQ formulations at 5, 10, 20, 30, 40 and 50% oil content. The mean values for each data type were labelled on top of the bars. Data were presented as mean ± SD (n = 3). *Significant compared to the mean particle size of other formulations with different oil content ($p < 0.05$). [a]Significant compared to the mean PDI value of 5% oil content formulations ($p < 0.05$). [b]Significant compared to the mean PDI value of 10% oil content formulations ($p < 0.05$).

TEM images showed formation of spherical particles in the formulations (Fig. 3). The GCPQ micelles (Fig. 3a), which are the self-assembled polymeric nanoparticles containing no drug (control), were seen as a collection of very small

particles with a diameter of <30 nm. In contrast, DS-GCPQ were seen as heterogeneous with sizes between 9 and 100 nm in diameter. The overall size of the DS-GCPQ particles appeared bigger than the size of the GCPQ micelles with no drug, which could indicate the encapsulation of the drug by the GCPQ polymer, positioning the oil droplets at the core and increasing the size of the DS-GCPQ particles. However, DS-GCPQ particles in the images appeared smaller than the size detected using DLS. The shrunken nanoparticles might cause the smaller size due to the drying process of the sample before the imaging. Formulations at 40% and 50% oil content also showed the formation of heterogenous particle size in the range of between 300 and 500 nm in diameter (Fig. S2 in Supplementary Information). The particles were seen tightly packed together, especially in the 50% oil formulation. The reason was probably that more oil causing more particles to be formed by GCPQ up to a point where there was hardly free space for the particles to move around, which could explain the higher viscosity observed in higher oil content formulations.
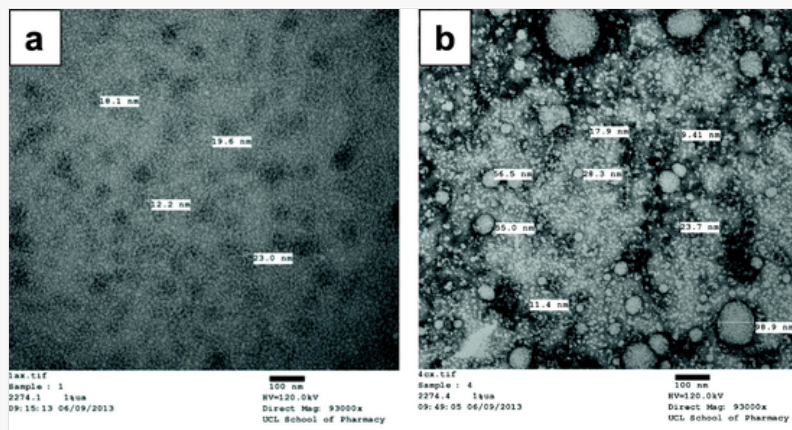
(i) Images are optimised for fast web viewing. Click on the image to view the original version.

Fig. 3

(a) GCPQ at 10 mg/ml in MilliQ water. The size of GCPQ micelles shown here is between 12 and 23 nm in diameter (93,000x magnification). (b) DS-GCPQ 1:10, 5% oil. The particle size was heterogeneous between 9 and 100 nm in diameter (93,000x magnification).

Due to the high DE%, small particle size and low PDI values, the DS-GCPQ nanoemulsion containing 5% oil content was chosen as the formulation to be used later on in the stability and cytotoxicity assays.

4.3 DsS-GepqCPQ stability

4.3.1 Stability in acidic and basic pH

No significant changes in particle size and PDI values in both DS-GCPQ and GCPQ suspensions when the formulations were adjusted into the highly acidic and basic environments when compared to the unaltered fresh preparation ($p > 0.05$) (Table 1). It was noticed that PDI values for GCPQ suspension were large ($0.4 - 0.6$), which might be due to the way the polymeric suspension was prepared in which the GCPQ suspension was not sonicated after completely dissolved in Milli-Q water compared to the DS-GCPQ formulations where they were sonicated to reach homogeneity. No aggregation was observed in all formulations that might have led to flocculation or cracking (phase separation) of the nanoemulsion, although it was expected to happen in the highly basic environment where the abundant presence of OH^- ions might neutralise the positively charged particles, leading to instability of the particle structure. The absence of aggregation is perhaps attributed to the highly charged GCPQ particles outweighing the effect of the counter ions introduced into the formulations.

Table 1

(i) The table layout displayed in this section is not how it will appear in the final version. The representation below is solely purposed for providing corrections to the table. To view the actual presentation of the table, please click on the Preview located at the top of the page.

The particle size and PDI values of GCPQ suspensions and DS-GCPQ in highly acidic and basic pH conditions.

	GCPQ			DS-GCPQ		
Condition	Fresh preparation	Acidic	Basic	Fresh preparation	Acidic	Basic

pH	4.53	1.73	11.10	4.40	1.67	10.90
Size (nm)	156.0 ± 1.2	152.6 ± 32.1	125.7 ± 13.1	195.7 ± 2.3	215.8 ± 0.7	192.2 ± 1.4
PDI	0.59 ± 0.15	0.46 ± 0.07	0.49 ± 0.06	0.24 ± 0.004	0.33 ± 0.01	0.24 ± 0.01

4.3.2 Stability in buffer

The results showed no significant decrease in DE% for formulations incubated in phosphate buffer (pH 6.8) for up to 4 h. Still, a significant decrease was seen in HCl buffer (pH 1.2), only at $t = 4$ h (Fig. 4a). Despite the presence of salts, the formulation was able to maintain its colloidal stability. It could be summarised that with the presence of 0.2 M salt in the acidic and neutral buffer, DS-GCPQ is stable and can withhold the drug encapsulation for as long as 2 and 4 h, respectively.

Fig. 4
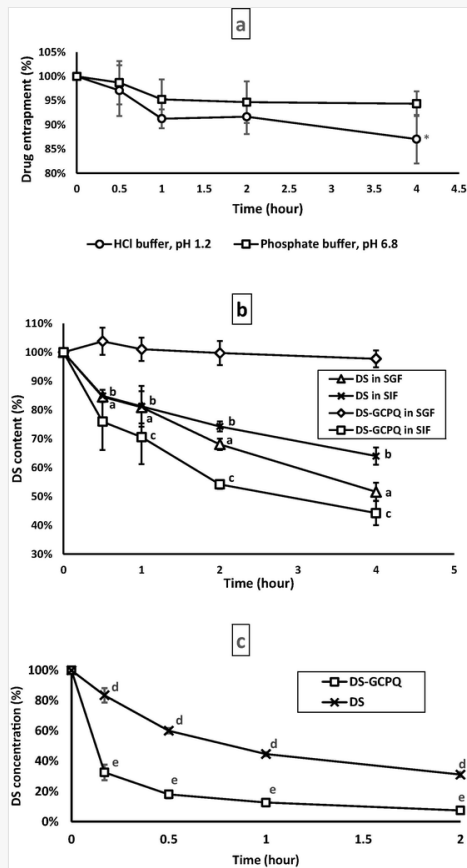
(a) DE% of DS-GCPQ in HCl and phosphate buffer at t = 0, 0.5, 1, 2 and 4 h. Buffers were at room temperature at the time of measurement (n = 3). *Significant compared to mean DE% at t = 0 h ($p < 0.05$). (b) The stability of DS following incubation of the DS-GCPQ formulation or the drug alone (control) in SGF and SIF up to 4 h at 37 °C. The drug concentration in the graph was normalised using percentages (n = 3). [a, b, c] Significant compared to drug content at t = 0 for DS in SGF, DS in SIF and DS-GCPQ in SIF, respectively ($p < 0.05$). (c) *In vitro* stability of DS and DS-GCPQ 5% oil upon incubation in diluted mouse plasma. The drug concentration in the graph was normalised using percentages. [d, e] Significant compared to drug entrapment at 0 h for DS and DS-GCPQ 5% oil, respectively ($p < 0.05$).

4.3.3 Stability in SGF and SIF

As shown in Fig. 4b, the stability of DS in SGF was improved greatly when it was incorporated with GCPQ with no significant degradation throughout the 4 h. In contrast, DS in DMSO (control) was significantly degraded over time. The improved stability of DS with GCPQ could indicate that the polymer protected the drug from the digesting activity of the pepsin enzyme and the low pH environment in the SGF. Meanwhile, in SIF, the DS content decreased gradually over time in both control and DS-GCPQ samples, probably due to the multiple enzymes affecting the structure of the

GCPQ polymers, causing the release of the encapsulated drug into the SIF and being degraded by the pancreatin enzyme.

4.3.4 Stability in mouse plasma

Fig. 4c shows the DS entrapment percentage derived from DS drug level analysis from plasma samples added with either DS solution in 0.5% DMSO or DS-GCPQ at 5% oil for 2-hour period. The result showed a significant decline in DS level in both groups, with a sharper drop seen in plasma with the nanoemulsions compared to plasma added with the naked DS. The $t_{1/2}$ for DS-GCPQ formulation and DS in DMSO was 7 min and 49 min, respectively. The plasma was diluted to reduce the activity of the protein and other endogenous components against the drug to see the rate of possible degradation of the drug upon contact with the plasma (Lalatsa et al., 2012a). The rapid decrease of DS level in the plasma added with DS-GCPQ formulation suggests the instability of the nanoparticle upon exposure to the components in the plasma. This instability had been observed previously when the formulations were incubated in the SIF, in which medium DS concentration was also decreased over time.

4.4 Activity of DsS-GepqCPQ against human pancreatic cancer cells

In the presence of copper ion, the IC_{50} for the DS group with or without GCPQ encapsulation were significantly lower than groups treated without copper (Fig. 5). This showed that copper highly enhanced the potency of DS in the cytotoxic activity against the MIAPaCa-2 cancer cell lines. This effect of copper on DS activity has been reported previously against melanoma, myeloma, and breast cancer cell lines (Chen et al., 2006; Chen and Dou, 2008; Conticello et al., 2012; Yip et al., 2011). A pattern of lower IC_{50} was also seen in groups treated with DS-GCPQ in comparison to the groups treated with DS but without GCPQ, although none of the differences was statistically significant. Cells treated with DS-GCPQ nanoemulsion and copper showed a remarkably low IC_{50}, almost 10 times the effect in cells treated with Cu + DS.

Fig. 5
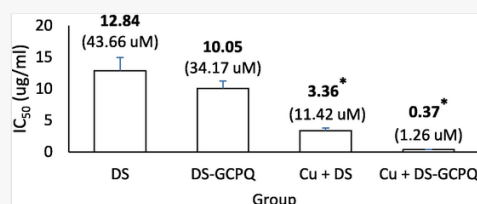
Summary of IC_{50} obtained from dose-response curves of four different treatments against MIAPaCa-2 cells. *Significant compared to IC_{50} of DS and DS-GCPQ ($p < 0.05$).

4.5 Pharmacokinetics of DsS-GepqCPQ

A developed and validated LC-MS/MS method was used to determine the pharmacokinetic profile of DS in mouse plasma upon IV administration of DS-GCPQ. MeDDC is the hydrophobic form of DS metabolite and was utilised in the chromatographic analysis as the marker for metabolised DS. The use of a cold stabilising agent to minimise the rapid degradation of DS in plasma samples for analytical measurement was first attempted by Johansson (1988), and later on, Zhang et al. (2013) modified the stabilising agent formula for a more practical approach in the sample preparation. DTPA was used to chelate plasma protein-bound cupric ions and to acidify the plasma to stop the interference of various thiols against DS stability in blood.

In this study, no IV DS control group (non-encapsulated) is to be used as a comparison to the IV formulation group since humans routinely take DS through oral routes only. DS-GCPQ at 20% oil (4 mg/ml DS) was used in the dosing regimen as this formulation had the highest viscosity suitable for parenteral injection through the mouse tail vein without causing high back pressure. The plasma concentration–time profile of the single IV administration of the formulation is shown in Fig. 6. Qualitative visual examination of the graph showed a gradual decline of concentration for both analytes within 1-hour post-injection. Plasma DS level continuously decreased until the end of the observation period at t = 2 h. MeDDC level was however seen to increase again starting from t = 1 h onwards. The pharmacokinetic parameters for IV administration of DS-GCPQ are shown in Table 2. Despite the gradual decline of the drug level, DS $t_{1/2}$ at 17 mins was longer than previously reported (6 mins) for IV administration (Liu et al., 2014).

Fig. 6
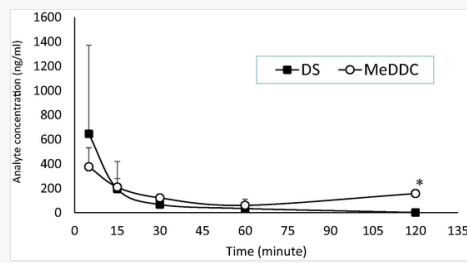
Plasma concentration–time profile of DS-GCPQ at 20% oil in 5% glucose IV treatment. Data were presented as mean ± SD (n = 5). * MeDDC was significantly higher compared to DS level at t = 2 h ($p < 0.05$).

Table 2

ⓘ The table layout displayed in this section is not how it will appear in the final version. The representation below is solely purposed for providing corrections to the table. To view the actual presentation of the table, please click on the [Preview] located at the top of the page.

Pharmacokinetic parameters of DS-GCPQ following single IV administration of the nanoemulsion to the animals.

Parameter	Unit	DS-GCPQ	
		DS	MeDDC
$t_{1/2}$	min	17	110
T_{max}	min	5	5
C_{max}	ng/ml	645.59	376.57
AUC_{0-2hr}	ng/ml.min	13348.47	16883.17

4.6 Anticancer study of DsS-GcpqCPQ

Treatments were started on Day 8 when the palpable tumour in mice reached approximately 6 to 7 mm in diameter and ended on Day 26, which was equivalent to the total amount of 10 IV injections given to the animals in the IV DS-GCPQ + Oral Cu group. The median survival time for animals received IV DS-GCPQ + Oral Cu, Oral DS + Oral Cu and control group was 30, 32 and 25 days, respectively (Fig. 7). Statistically, the median survival time in animals received no treatment (control) was significantly shorter compared to the values in both IV DS-GCPQ + Oral Cu and Oral DS + Oral Cu treatment groups (P_{l2} = 0.0305, P_{l2} = 0.0031, respectively). There was no significant difference in the survival time between the two treatment groups. Bodyweight change for each animal in all groups also showed no significant difference upon tumour implantation and administration of the treatments. It is suggested that the tumour burden did not induce severe health deterioration effects, and the treatments did not produce toxicity or any adverse side effects on the animals. All tumours, with or without treatments, showed a gradual increase in tumour volume over time (Fig. S3 in Supplementary Information).

ⓘ Images are optimised for fast web viewing. Click on the image to view the original version.

Fig. 7
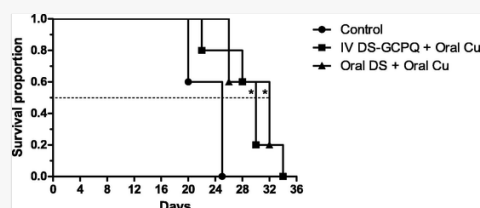
Kaplan-Meier survival curve of nude mice bearing pancreatic xenograft tumours. *Median survival for IV DS-GCPQ + Oral Cu and Oral DS + Oral Cu group was significantly different compared to the control ($p < 0.05$).

The analysis of animal survival is commonly used to measure clinical outcomes. Since the humane practice of the experiment only allows the animals to bear a single tumour up to a certain size (maximum of 13 mm in diameter for the

present case), this was used as a surrogate marker and an endpoint to study the anticancer effects of DS-GCPQ nanoemulsion. Based on this modified survival study, the treatment of DS with copper supplementation significantly increased the survival of the animals bearing MIAPaCa-2 xenograft pancreatic tumours. It has been shown that both oral and IV treatment of DS produced the effect of tumour growth suppression, rendering the IV route the less preferable choice for the route of administration of the drug. The method of administering DS in soybean oil is however only feasible in this experiment for easy oral administration of DS via oral gavage to the mice. This approach is less desirable in humans as the drug is more convenient and commonly taken in the solid form of capsules or tablets.

5 Discussion

GCPQ with higher palmitoylation (more apolar polymers) allows a higher hydrophobic drug entrapment, as previously occurred in other GCPQ nanoparticle formulations (Qu et al., 2006). Therefore, the hypothesis is that using a highly hydrophobic vehicle or excipient to encapsulate drugs, such as oil, would give a possibility of high drug entrapment upon formulation with the polymer. DS-GCPQ was able to be loaded with as high as 50% oil v/v without disrupting the colloidal stability of the formulation. In theory, the disperse phase of an emulsion can occupy up to 74% of the phase volume, but common pharmaceutical emulsions usually contain only between 10 and 30% of the disperse phase (Eccleston, 2013). Therefore, it is suggested that GCPQ at 19.9% palmitoylation is a good emulsifier as it can withhold such amount of oil, which is generally high compared to other commercially available emulsions. The high positive-charge values of DS-GCPQ nanoparticles at an acidic pH of 5 were probably contributed by the GCPQ hydrophilic substituent, the trimethyl ammonium groups (Uchegbu et al., 2004). The stable condition of the formulations in various pH and buffers might also be due to the high positive-charge values, as the strong charges around the individual particles continuously repel each other and ensure the dispersion stability of the formulations by avoiding aggregation or flocculation.

The aim of the present study was to improve the delivery system of DS for anticancer purposes by developing a nanoparticle formulation that uses GCPQ polymer to incorporate the drug. Thus, step-by-step DS-GCPQ formulation development was conducted by considering that the final, optimised formulation could be administered orally or intravenously. The initial work focused on developing DS-GCPQ into an oral formulation as oral administration is a more convenient, cost-effective and commonly used route of administration. The pharmacokinetic profile of DS-GCPQ when administered orally, however, showed a low level of DS concentration in the blood (data not included). Henceforth, the focus of the study shifted to developing the DS-GCPQ formulation towards intravenous administration purposes.

Nanoparticles tend to be covered with protein corona upon contact with biological mediums. In blood, different biological molecules, of which majority are proteins and small portions of lipids, compete to adsorb onto the surface of nanoparticles. Albumin, fibrinogen, apolipoprotein and immunoglobulin G are the most commonly present in the corona as they are highly abundant in the blood plasma (Aggarwal et al., 2009). The protein adsorption to the nanoparticles also promotes configuration change to the particle's surface morphology. The formation of protein corona around DS-GCPQ particles could have changed their physicochemical properties and might have contributed to the instability of the nanoemulsion in the plasma. The protein corona could alter the size and surface composition of the nanoparticles, thus giving a new biological identity to the nanoparticles which could trigger physiological responses such as agglomeration, as well as affecting the transport, circulation lifetime and toxicity of the nanoparticles (Nierenberg et al., 2018).

The corona's structure and composition depend on the nanomaterials' physicochemical properties (e.g. size, shape, surface charge and duration of exposure) (Rahman et al., 2013). The protein corona formation is however not permanently fixed, and composition is due to change depending on the kinetic rate of the adsorption and desorption of the protein, as well as upon movement of particles from one site to the other, such as from the blood circulation into the tissue. The change in corona's composition could also be due to the different relative abundance of different types of protein in the biological environment. The effects of protein corona suggest that the DS-GCPQ nanoparticle behaviour from *in vitro* data does not necessarily predict the same activity happening *in vivo* for the same nanoparticles.

The decrease in DS level upon exposure to the mouse plasma might also be attributed to the action of the mononuclear phagocytic system (MPS) eliminating the nanoparticles. Positively charged nanoparticles were reported to have a higher rate of opsonisation by the phagocytes compared to ones with neutral charges (Nandhakumar et al., 2017). In future studies, perhaps one possible way to improve the stability of DS-GCPQ nanoparticles is to attach shielding group on the particle surface to block electrostatic and hydrophobic attractions of opsonins from binding to the particles, such as attaching biodegradable poly(ethylene glycol) (PEG) chains to avoid the MPS elimination (Chong et al., 2021).

The high AUC value of DS from the IV administration (13348.471 ng/ml.min) was expected as the nanoparticles avoided the first-pass metabolism in the liver. The other possible explanation is less deposition of DS-GCPQ in major organs, which increases the drug level in blood circulation. Serrano et al. (2015) revealed that very low levels of GCPQ nanoparticles had been found in the liver and none in the spleen following an IV administration. A slight elevation of

MeDDC level, which was higher than the DS level at time point 120 min, might be due to the late release of DS from some of the nanoparticles, causing parts of the administered DS to be converted into MeDDC in the liver at a later time than the rest of the drug.

The effectiveness of DS in suppressing the growth of pancreatic cancer xenografts has been reported by Han et al. (2013). In the study, DS and copper were made into a complex and administered intraperitoneally to animals with subcutaneous pancreatic tumour xenograft, which was able to inhibit 62.8% tumour growth when compared to the control. The positive effect of DS against pancreatic tumour growth was also achieved when administered in combination with other active ingredients, such as gemcitabine (Dalla Pozza et al., 2011; Kim et al., 2013), and arsenic trioxide with ascorbic acid (Dinnen et al., 2013). Copper is an essential ingredient in elevating the anticancer property of DS. Since there was a lack of information on the possible interactions between the copper ions and the particles of the nanoemulsions in the blood microenvironment, the copper was administered orally in the form of copper gluconate. Copper (cupric) gluconate is a widely available salt as a dietary supplement and is one of the Generally Regarded as Safe (GRAS) substances. Copper gluconate has also been used in Phase 1 clinical trials to study DS against hepatic metastases from solid tumours (ClinicalTrials.gov Identifier NCT00742911). As copper can form complexes with DS *in vivo* (Johansson, 1992), it is possible that copper and DS form complexes in the tissues (e.g., liver) and the tumours. The accumulation of copper in cancer cells is high (Oliveri, 2022). The supplementation of copper gluconate was therefore assumed to help increase copper's bioavailability in blood circulation and the tumour microenvironment, thus aiding the anticancer activity of the DS-GCPQ without causing unnecessary toxicity from the copper overdose.

Several reported mechanisms of actions responsible for the anticancer effect of DS include inhibition of nuclear factor kappa B (NF-κB) (Liu et al., 2014; Wang et al., 2003), blocking the activity of P-glycoprotein membrane pump (Loo et al., 2004), induction of apoptosis (Cen et al., 2004; Li et al., 2018a; Shah O'Brien et al., 2019) and reduction of angiogenesis and metastasis (Li et al., 2018b; Shian et al., 2003). The enhanced cytotoxicity effect of DS with copper appears to happen by inhibiting the proteasome pathway leading to the induction of apoptosis activities in human cancer cell lines (Chen et al., 2006). These DS activities hence provide enough evidence to repurpose the use of DS as an adjuvant anticancer agent. Additionally, as DS is an old generic drug, the drug is inexpensive, easily available and has negligible adverse effects compared to classical chemotherapeutic drugs. The utilisation of GCPQ to create a robust DS formulation for efficient drug delivery can also avoid the expensive and time-consuming development process of new anticancer drugs that involves costly pre-clinical and clinical testings.

6 Conclusion

DS-GCPQ nanoemulsion protected the drug in the blood circulation to some extent and delivered the drug load to the tumour site. An additional feature of the nanoemulsion was the ability to be loaded with high amount of oil, thus, the high amount of drug can also be encapsulated within the nanoparticles without compromising the colloidal stability of the formulation. The high loading capacity of DS-GCPQ nanoemulsion could enable the administration of high DS concentrations that could reach the therapeutic dose needed for cancer treatment without the risk of toxicity from the use of high surfactant/emulsifier in the formulation. This study proves the potential of the newly found DS-GCPQ nanoemulsions to be used and developed further for cancer therapeutic purposes.

7 Data availability

Data will be made available on request.

Q4 Uncited reference

Faiman et al. (1983).

CRediT authorship contribution statement

Erazuliana Abd Kadir : Methodology, Investigation, Validation, Formal analysis, Writing – original draft, Writing – review & editing, Visualization, Funding acquisition. **Ijeoma F. Uchegbu :** Supervision. **Andreas G. Schätzlein :** Validation, Resources, Writing – review & editing, Supervision, Project administration, Funding acquisition.

Declaration of Competing Interest

The authors declare that they have no known competing financial interests or personal relationships that could have appeared to influence the work reported in this paper.

Acknowledgements

Appendix A Supplementary material

Supplementary data to this article can be found online at https://doi.org/10.1016/j.ijpharm.2023.123036.

References

> ⓘ The corrections made in this section will be reviewed and approved by a journal production editor. The newly added/removed references and its citations will be reordered and rearranged by the production team.

Aggarwal, P., Hall, J.B., McLeland, C.B., Dobrovolskaia, M.A., McNeil, S.E., 2009. Nanoparticle interaction with plasma proteins as it relates to particle biodistribution, biocompatibility and therapeutic efficacy. Adv. Drug Deliv. Rev. 61, 428–437. doi:10.1016/j.addr.2009.03.009.

Cen, D., Brayton, D., Shahandeh, B., Meyskens, F.L., Jr., Farmer, P.J., 2004. Disulfiram facilitates intracellular Cu uptake and induces apoptosis in human melanoma cells. J. Med. Chem. 47, 6914–6920. doi:10.1021/jm049568z.

Chen, D., Cui, Q.C., Yang, H., Dou, Q.P., 2006. Disulfiram, a clinically used anti-alcoholism drug and copper-binding agent, induces apoptotic cell death in breast cancer cultures and xenografts via inhibition of the proteasome activity. Cancer Res. 66, 10425–10433. doi:10.1158/0008-5472.can-06-2126.

Chen, D., Dou, Q.P., 2008. New uses for old copper-binding drugs: converting the pro-angiogenic copper to a specific cancer cell death inducer. Expert Opin. Ther. Targets 12, 739–748. doi:10.1517/14728222.12.6.739.

Chick, J., 1999. Safety issues concerning the use of disulfiram in treating alcohol dependence. Drug Saf. 20, 427–435. doi:10.2165/00002018-199920050-00003.

Chong, W.M., Lim, V., Abd Kadir, E., 2021. Hydrophobically modified PEGylated glycol chitosan nanoparticles: synthesis, characterisation and anticancer properties. New J. Chem. 45, 11359–11370. doi:10.1039/D1NJ01710A.

Conticello, C., Martinetti, D., Adamo, L., Buccheri, S., Giuffrida, R., Parrinello, N., Lombardo, L., Anastasi, G., Amato, G., Cavalli, M., Chiarenza, A., De Maria, R., Giustolisi, R., Gulisano, M., Di Raimondo, F., 2012. Disulfiram, an old drug with new potential therapeutic uses for human hematological malignancies. Int. J. Cancer 131, 2197–2203. doi:10.1002/ijc.27482.

Dalla Pozza, E., Donadelli, M., Costanzo, C., Zaniboni, T., Dando, I., Franchini, M., Arpicco, S., Scarpa, A., Palmieri, M., 2011. Gemcitabine response in pancreatic adenocarcinoma cells is synergistically enhanced by dithiocarbamate derivatives. Free Radical Biol. Med. 50, 926–933. doi:10.1016/j.freeradbiomed.2011.01.001.

Dinnen, R.D., Mao, Y., Qiu, W., Cassai, N., Slavkovich, V.N., Nichols, G., Su, G.H., Brandt-Rauf, P., Fine, R.L., 2013. Redirecting apoptosis to aponecrosis induces selective cytotoxicity to pancreatic cancer cells through increased ROS, decline in ATP levels, and VDAC. Mol Cancer Ther. 12, 2792–2803. doi:10.1158/1535-7163.mct-13-0234.

Duan, L., Shen, H., Zhao, G., Yang, R., Cai, X., Zhang, L., Jin, C., Huang, Y., 2014. Inhibitory effect of disulfiram/copper complex on non-small cell lung cancer cells. Biochem. Biophys. Res. Commun. 446, 1010–1016. doi:10.1016/j.bbrc.2014.03.047.

Eccleston, G.M., 2013. Emulsions and creams. In: Aulton, M.E., Taylor, K.M.G. (Eds.), Aulton's Pharmaceutics; The Design and Manufacture of Medicines, Fourth ed. Churchill Livingstone, pp. 436–464.

Eneanya, D.I., Bianchine, J.R., Duran, D.O., Andresen, B.D., 1981. The actions of metabolic fate of disulfiram. Annu. Rev. Pharmacol. Toxicol. 21, 575–596. doi:10.1146/annurev.pa.21.040181.003043.

Faiman, M.D., Artman, L., Maziasz, T., 1983. Diethyldithiocarbamic acid methyl ester distribution, elimination, and LD50 in the rat after intraperitoneal administration. Alcohol.: Clin. Exp. Res. 7, 307–311. doi:10.1111/j.1530-0277.1983.tb05466.x.

Ginestier, C., Hur, M.H., Charafe-Jauffret, E., Monville, F., Dutcher, J., Brown, M., Jacquemier, J., Viens, P., Kleer, C.G., Liu, S., Schott, A., Hayes, D., Birnbaum, D., Wicha, M.S., Dontu, G., 2007. ALDH1 is a marker of normal and malignant human mammary stem cells and a predictor of poor clinical outcome. Cell Stem Cell 1, 555–567. doi:10.1016/j.stem.2007.08.014.

Han, J., Liu, L., Yue, X., Chang, J., Shi, W., Hua, Y., 2013. A binuclear complex constituted by diethyldithiocarbamate and copper(I) functions as a proteasome activity inhibitor in pancreatic cancer cultures and xenografts. Toxicol. Appl. Pharmacol. 273, 477–483. doi:10.1016/j.taap.2013.09.009.

Jiang, F., Qiu, Q., Khanna, A., Todd, N.W., Deepak, J., Xing, L., Wang, H., Liu, Z., Su, Y., Stass, S.A., Katz, R.L., 2009. Aldehyde dehydrogenase 1 is a tumor stem cell-associated marker in lung cancer. Mol. Cancer Res. 7, 330-338. Doi:10.1158%2F1541-7786.MCR-08-0393.[Instruction: The word 'Doi' for several references (Jiang, F. et al.; Nechutsa, H., et al.; Rahman, M., et al.; and Shah O'Brien, p., et al.) are spelled with capitalised D. I think it should be changed to non-capitalised 'd' to make them same as the others.]

Johansson, B., 1988. Stabilization and quantitative determination of disulfiram in human plasma samples. Clin. Chim. Acta 177, 55–63. doi:10.1016/0009-8981(88)90307-5.

Johansson, B., 1992. A review of the pharmacokinetics and pharmacodynamics of disulfiram and its metabolites. Acta Psychiatr. Scand. 86, 15–26. doi:10.1111/j.1600-0447.1992.tb03310.x.

Kannappan, V., Ali, M., Small, B., Rajendran, G., Elzhenni, S., Taj, H., Wang, W., Dou, Q.P., 2021. Recent advances in repurposing disulfiram and disulfiram derivatives as copper-dependent anticancer agents. Front. Mol. Biosci. 8, 741316. doi:10.3389/fmolb.2021.741316.

Kim, S.K., Kim, H., Lee, D.H., Kim, T.S., Kim, T., Chung, C., Koh, G.Y., Kim, H., Lim, D.S., 2013. Reversing the intractable nature of pancreatic cancer by selectively targeting ALDH-high, therapy-resistant cancer cells. PLoS One 8, e78130.

Lalatsa, A., Garrett, N.L., Ferrarelli, T., Moger, J., Schatzlein, A.G., Uchegbu, I.F., 2012a. Delivery of peptides to the blood and brain after oral uptake of quaternary ammonium palmitoyl glycol chitosan nanoparticles. Mol. Pharmaceutics 9, 1764–1774. doi:10.1021/mp300068j.

Lalatsa, A., Lee, V., Malkinson, J.P., Zloh, M., Schatzlein, A.G., Uchegbu, I.F., 2012b. A prodrug nanoparticle approach for the oral delivery of a hydrophilic peptide, leucine(5)-enkephalin, to the brain. Mol. Pharmaceutics 9, 1665–1680. doi:10.1021/mp300009u.

Lalatsa, A., Schatzlein, A.G., Garrett, N.L., Moger, J., Briggs, M., Godfrey, L., Iannitelli, A., Freeman, J., Uchegbu, I.F., 2015. Chitosan amphiphile coating of peptide nanofibres reduces liver uptake and delivers the peptide to the brain on intravenous administration. J. Controlled Release 197, 87–96. doi:10.1016/j.jconrel.2014.10.028.

Li, Y., Shen, J., Fang, M., Huang, X., Yan, H., Jin, Y., Li, J., Li, X., 2018a. The promising antitumour drug disulfiram inhibits viability and induces apoptosis in cardiomyocytes. Biomed. Pharmacother. 108, 1062–1069. doi:10.1016/j.biopha.2018.09.123.

Li, Y., Wang, L.H., Zhang, H.T., Wang, Y.T., Liu, S., Zhou, W.L., Yuan, X.Z., Li, T.Y., Wu, C.F., Yang, J.Y., 2018b. Disulfiram combined with copper inhibits metastasis and epithelial-mesenchymal transition in hepatocellular carcinoma through the NF-κB and TGF-β pathways. J. Cell. Mol. Med. 22, 439–451. doi:10.1111/jcmm.13334.

Lin, J., Haffner, M.C., Zhang, Y., Lee, B.H., Brennen, W.N., Britton, J., Kachhap, S.K., Shim, J.S., Liu, J.O., Nelson, W.G., Yegnasubramanian, S., Carducci, M.A., 2011. Disulfiram is a DNA demethylating agent and inhibits prostate cancer cell growth. Prostate 71, 333–343. doi:10.1002/pros.21247.

Liu, P., Wang, Z., Brown, S., Kannappan, V., Tawari, P.E., Jiang, W., Irache, J.M., Tang, J.Z., Armesilla, A.L., Darling, J.L., Tang, X., Wang, W., 2014. Liposome encapsulated Disulfiram inhibits NFκB pathway and targets breast cancer stem cells in vitro and in vivo. Oncotarget 5, 7471–7485. doi:10.18632/oncotarget.2166.

Loo, T.W., Bartlett, M.C., Clarke, D.M., 2004. Disulfiram metabolites permanently inactivate the human multidrug resistance P-glycoprotein. Mol. Pharmaceutics 1, 426–433. doi:10.1021/mp049917l.

Marcato, P., Dean, C.A., Giacomantonio, C.A., Lee, P.W., 2011. Aldehyde dehydrogenase: its role as a cancer stem cell marker comes down to the specific isoform. Cell Cycle 10, 1378–1384. doi:10.4161/cc.10.9.15486.

Meraz-Torres, F., Plöger, S., Garbe, C., Niessner, H., Sinnberg, T., 2020. Disulfiram as a therapeutic agent for metastatic malignant melanoma - old myth or new logos? Cancers 12. doi:10.3390/cancers12123538.

Nandhakumar, S., Dhanaraju, M.D., Sundar, V.D., Heera, B., 2017. Influence of surface charge on the in vitro protein adsorption and cell cytotoxicity of paclitaxel loaded poly(ε-caprolactone) nanoparticles. Bull. Fac. Pharm. (Cairo Univ.) 55, 249–258. doi:10.1016/j.bfopcu.2017.06.003.

Nechushtan, H., Hamamreh, Y., Nidal, S., Gotfried, M., Baron, A., Shalev, Y.I., Nisman, B., Peretz, T., Peylan-Ramu, N., 2015. A phase IIb trial assessing the addition of disulfiram to chemotherapy for the treatment of metastatic non-small cell lung cancer. Oncologist 20, 366-367. Doi:10.1634%2Ftheoncologist.2014-0424.

Nierenberg, D., Khaled, A.R., Flores, O., 2018. Formation of a protein corona influences the biological identity of nanomaterials. Rep. Pract. Oncol. Radiother. 23, 300–308. doi:10.1016/j.rpor.2018.05.005.

Oliveri, V., 2022. Selective targeting of cancer cells by copper ionophores: An overview. Front. Mol. Biosci. 9. doi:10.3389/fmolb.2022.841814.

Qu, X., Khutoryanskiy, V.V., Stewart, A., Rahman, S., Papahadjopoulos-Sternberg, B., Dufes, C., McCarthy, D., Wilson, C.G., Lyons, R., Carter, K.C., Schatzlein, A., Uchegbu, I.F., 2006. Carbohydrate-based micelle clusters which enhance hydrophobic drug bioavailability by up to 1 order of magnitude. Biomacromolecules 7, 3452–3459. doi:10.1021/bm0604000.

Qu, Y., Li, A., Ma, L., Iqbal, S., Sun, X., Ma, W., Li, C., Zheng, D., Xu, Z., Zhao, Z., Ma, D., 2021. Nose-to-brain delivery of disulfiram nanoemulsion in situ gel formulation for glioblastoma targeting therapy. Int. J. Pharm. 597, 120250. doi:10.1016/j.ijpharm.2021.120250.

Rahman, M., Laurent, S., Tawil, N., Yahia, L.H., Mahmoudi, M., 2013. Nanoparticle and Protein Corona, in: Rahman, M., Laurent, S., Tawil, N., Yahia, L.H., Mahmoudi, M. (Eds.), Protein-Nanoparticle Interactions: The Bio-Nano Interface. Springer Berlin Heidelberg, Berlin, Heidelberg, pp. 21-44. Doi:10.1007/978-3-642-37555-2_2.

Rasheed, Z.A., Yang, J., Wang, Q., Kowalski, J., Freed, I., Murter, C., Hong, S.M., Koorstra, J.B., Rajeshkumar, N.V., He, X., Goggins, M., Iacobuzio-Donahue, C., Berman, D.M., Laheru, D., Jimeno, A., Hidalgo, M., Maitra, A., Matsui, W., 2010. Prognostic significance of tumorigenic cells with mesenchymal features in pancreatic adenocarcinoma. J. Natl. Cancer Inst. 102, 340–351. doi:10.1093/jnci/djp535.

Seitz, H.K., Stickel, F., 2007. Molecular mechanisms of alcohol-mediated carcinogenesis. Nat. Rev. Cancer 7, 599. doi:10.1038/nrc2191.

Serrano, D.R., Lalatsa, A., Dea-Ayuela, M.A., Bilbao-Ramos, P.E., Garrett, N.L., Moger, J., Guarro, J., Capilla, J., Ballesteros, M.P., Schätzlein, A.G., Bolás, F., Torrado, J.J., Uchegbu, I.F., 2015. Oral particle uptake and organ targeting drives the activity of amphotericin B nanoparticles. Mol. Pharmaceutics 12, 420–431. doi:10.1021/mp500527x.

Shah O'Brien, P., Xi, Y., Miller, J.R., Brownell, A.L., Zeng, Q., Yoo, G.H., Garshott, D.M., O'Brien, M.B., Galinato, A.E., Cai, P., Narula, N., Callaghan, M.U., Kaufman, R.J., Fribley, A.M., 2019. Disulfiram (Antabuse) activates ROS-dependent ER stress and apoptosis in oral cavity squamous cell carcinoma. J. Clin. Med. 8, 611. Doi:10.3390%2Fjcm8050611.

Shian, S.G., Kao, Y.R., Wu, F.Y., Wu, C.W., 2003. Inhibition of invasion and angiogenesis by zinc-chelating agent disulfiram. Mol. Pharmacol. 64, 1076–1084. doi:10.1124/mol.64.5.1076.

Siew, A., Le, H., Thiovolet, M., Gellert, P., Schatzlein, A., Uchegbu, I., 2012. Enhanced oral absorption of hydrophobic and hydrophilic drugs using quaternary ammonium palmitoyl glycol chitosan nanoparticles. Mol. Pharmaceutics 9, 14–28. doi:10.1021/mp200469a.

Sung, H., Ferlay, J., Siegel, R.L., Laversanne, M., Soerjomataram, I., Jemal, A., Bray, F., 2021. Global Cancer Statistics 2020: GLOBOCAN Estimates of Incidence and Mortality Worldwide for 36 Cancers in 185

Countries. CA Cancer J. Clin. 71, 209–249. doi:10.3322/caac.21660.

Swetha, K.L., Sharma, S., Chowdhury, R., Roy, A., 2020. Disulfiram potentiates docetaxel cytotoxicity in breast cancer cells through enhanced ROS and autophagy. Pharmacol. Rep. 72, 1749–1765. doi:10.1007/s43440-020-00122-1.

Uchegbu, I.F., Sadiq, L., Arastoo, M., Gray, A.I., Wang, W., Waigh, R.D., Schatzlein, A.G., 2001. Quaternary ammonium palmitoyl glycol chitosan–a new polysoap for drug delivery. Int. J. Pharm. 224, 185–199. doi:10.1016/s0378-5173(01)00763-3.

Uchegbu, I.F., Sadiq, L., Pardakhty, A., El-Hammadi, M., Gray, A.I., Tetley, L., Wang, W., Zinselmeyer, B.H., Schätzlein, A.G., 2004. Gene transfer with three amphiphilic glycol chitosans—the degree of polymerisation is the main controller of transfection efficiency. J. Drug Targeting 12, 527–539. doi:10.1080/10611860400011943.

Wang, W., McLeod, H.L., Cassidy, J., 2003. Disulfiram-mediated inhibition of NF-κB activity enhances cytotoxicity of 5-fluorouracil in human colorectal cancer cell lines. Int. J. Cancer 104, 504–511. doi:10.1002/ijc.10972.

Wright, C., Moore, R.D., 1990. Disulfiram treatment of alcoholism. Am. J. Med. 88, 647–655. doi:10.1016/0002-9343(90)90534-K.

Xu, Y., Lu, L., Luo, J., Wang, L., Zhang, Q., Cao, J., Jiao, Y., 2021. Disulfiram alone functions as a radiosensitizer for pancreatic cancer both in vitro and in vivo. Front. Oncol. 11. doi:10.3389/fonc.2021.683695.

Yang, S., Han, Y., Bao, B., Hu, C., Li, Z., 2022. Boosting the anti-tumor performance of disulfiram against glioblastoma by using ultrasmall nanoparticles and HIF-1α inhibitor. Compos. B 243, 110117. doi:10.1016/j.compositesb.2022.110117.

Yip, N.C., Fombon, I.S., Liu, P., Brown, S., Kannappan, V., Armesilla, A.L., Xu, B., Cassidy, J., Darling, J.L., Wang, W., 2011. Disulfiram modulated ROS-MAPK and NFκB pathways and targeted breast cancer cells with cancer stem cell-like properties. Br. J. Cancer 104, 1564–1574. doi:10.1038/bjc.2011.126.

Zhang, H., Chen, D., Ringler, J., Chen, W., Cui, Q.C., Ethier, S.P., Dou, Q.P., Wu, G., 2010. Disulfiram treatment facilitates phosphoinositide 3-kinase inhibition in human breast cancer cells in vitro and in vivo. Cancer Res. 70, 3996–4004. doi:10.1158/0008-5472.can-09-3752.

Zhang, L., Jiang, Y., Jing, G., Tang, Y., Chen, X., Yang, D., Zhang, Y., Tang, X., 2013. A novel UPLC-ESI-MS/MS method for the quantitation of disulfiram, its role in stabilized plasma and its application. J. Chromatogr. B: Anal. Technol. Biomed. Life Sci. 937, 54–59. doi:10.1016/j.jchromb.2013.08.009.

Graphical abstract

Images are optimised for fast web viewing. Click on the image to view the original version.
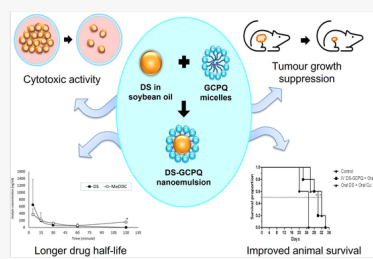
Appendix A Supplementary material

The following are the Supplementary data to this article:

📄 [Multimedia Component 1](#)

Supplementary data 1

Queries and Answers

Q1

Query: Please review the **given names and surnames** to make sure that we have identified them correctly and that they are presented in the desired order. Carefully verify the spelling of all authors' names as well. If changes are needed, please provide the edits in the author section. /

Answer: Reviewed

Q2

Query: Your article is being processed as a regular item to be included in a regular issue. Please confirm if this is correct or if your article should be published in a special issue using the responses below. /

Answer: Yes

Q3

Query: Ref(s). 'Scientific Acts 1986' is/are cited in the text but not provided in the reference list. Please provide it/them in the reference list or delete these citations from the text. /

Answer: The sentence without the appropriate citation has been removed.

Q4

Query: The **Uncited References** section comprises references that occur in the reference list but are not available in the body of the article text. Please cite each reference in the text or, alternatively, delete it. Any reference not dealt with will be retained in this section. /

Answer: Done

Q5

Query: Correctly acknowledging the primary **funders and grant IDs** of your research is important to ensure compliance with funder policies. Please make sure that funders are mentioned accordingly. /

Answer: Reviewed